0026-895X/96/010030-10$3.00/0
Copyright © by The American Society for Pharmacology and Experimental Therapeutics
All rights of reproduction in any form reserved.
MOLECULAR PHARMACOLOGY, 49:30–39 (1996).

MOL PHARM

Coexpression of β1 with Cardiac Sodium Channel α Subunits in Oocytes Decreases Lidocaine Block

JONATHAN C. MAKIELSKI,[1] JAMES T. LIMBERIS, STEVEN Y. CHANG, ZHENG FAN,[1] and JOHN W. KYLE

The Cardiac Electrophysiology Laboratories, The University of Chicago, Chicago, Illinois 60637

Received May 16, 1995; Accepted October 8, 1995

SUMMARY

Coexpression of the rat β1 subunit with rat brain and skeletal muscle sodium channel α subunits in *Xenopus* oocytes normalizes currents by accelerating sodium current decay kinetics, shifting steady state availability relationships, and accelerating recovery from inactivation. Unlike brain and skeletal muscle, the heart α subunit expressed without β1 has native-like decay kinetics in oocytes. Messenger RNA for β1 has been found in heart, but whether and how it affects cardiac sodium channel function are unclear. We studied coexpression of human heart α subunit with β1 in *Xenopus* oocytes using two microelectrode voltage-clamp and macropatch techniques. Coexpression with β1 caused a significant positive shift of 3–7 mV in the midpoint of the steady state inactivation relationship but did not affect single-channel conductance, activation, current decay, or recovery from inactivation. Sensitivity to lidocaine block, however, was decreased for both resting state block (K_d = 0.5–1.3 mM) and phasic block in response to pulse trains, but inactivated state block was not affected (K_d = ~10 μM). Coexpression with β1 increased the rate of recovery from lidocaine block, which accounted for the major part of the observed differences in tonic and phasic block. A β1 construct with the cytoplasmic tail removed also produced these effects, demonstrating that the β1 cytoplasmic tail was not involved in altering lidocaine block. We conclude that the β1 subunit is capable of affecting function of the cardiac sodium channel in oocytes by decreasing tonic and phasic lidocaine block with small effects on gating.

At least some voltage-gated sodium ion channels are heterodimers, composed of an α subunit (240–300 kDa), β1 subunit(s) (33–39 kDa), and/or β2 subunits (33 kDa). Six distinct sodium channel α subunits have been identified by both cloning and expression. Several of these α subunits display abnormally slow kinetics when expressed alone in *Xenopus* oocytes. The β1 subunit of the voltage-gated sodium channels was first identified in brain and was also shown to be present in association with skeletal muscle sodium channels (for review, see Ref. 1). The β1 subunit mRNA was also detected in heart tissue (2, 3), and it has been localized to a single gene (4, 3). For brain and skeletal muscle channels expressed in oocytes, the β1 subunit accelerates the macroscopic decay of I_{Na} and shifts the steady state (conditioning durations <500 msec) voltage-dependent availability in the negative direction (5, 6), making these kinetics more closely resemble those found in native tissues. Unlike brain and skeletal muscle channels, cardiac sodium channel α subunits expressed alone in oocytes grossly resemble those in native tissues (7). Coexpression of β1 has been variably reported to have either no effect on decay kinetics, recovery from inactivation, or steady state availability (3) or to have accelerated decay and recovery and shift steady state availability (8). In the present study, we show that coexpression of a rat brain β1 subunit with an hH1a (9, 10) causes significant, albeit small effects, on sodium channel gating but has a greater effect to reduce channel block by the local anesthetic and antiarrhythmic lidocaine. To address possible mechanism, we also investigated β1 subunits mutated to delete the cytoplasmic tail.[2]

Materials and Methods

Sodium channel α and β1 subunit clones. The method of preparation of cRNA and *Xenopus* oocytes in our laboratory is standard and has been previously described (7). hH1a was kindly provided by Drs. H. Hartmann and A. M. Brown (Baylor University, Houston, TX). The rat brain β1 subunit was cloned from a rat brain poly(A)$^+$ RNA using RT-PCR. The DNA sequence exactly corre-

This work was supported by National Institutes of Health Grants PO1-HL20592 and HL56441 (J.C.M.) and an American Heart Association, Metropolitan Chicago Affiliate, Grant-in-Aid (J.W.K.). J.C.M. was an Established Investigator of the American Heart Association.

[1] Current affiliation: Department of Medicine, Cardiology Section, University of Wisconsin, Madison, Wisconsin.

[2] Some results were presented at the 1995 Biophysical Society Meeting (11).

ABBREVIATIONS: hH1a, human heart sodium channel isoform; RT-PCR, reverse transcriptase-polymerase chain reaction; βnt, β no tail; M-MLV, Maloney murine leukemia virus; GAPDH, glyceraldehyde-3-phosphate dehydrogenase; ANOVA, analysis of variance; HEPES, 4-(2-hydroxyethyl)-1-piperazineethanesulfonic acid; I_{Na}, sodium current; V_c, conditioning potential; t_c, duration of conditioning depolarization.

MOLECULAR PHARMACOLOGY
aspet
Downloaded from molpharm.aspetjournals.org at Zhejiang University on December 1, 2012

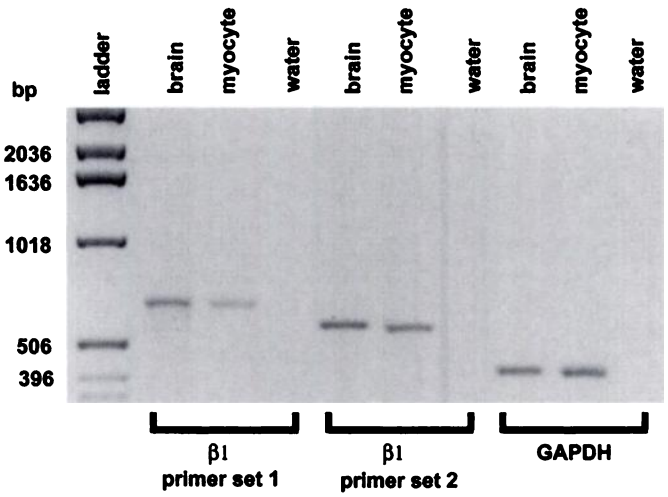

Fig. 1. β1 subunit mRNA is present in isolated cardiac myocytes. Total RNA isolated from rat brain, rat whole heart, or rat ventricular myocytes were assayed using RT-PCR for the presence of β1 mRNA. Then, 1 μg of total RNA was reverse transcribed with M-MLV RT to generate cDNA that was then subjected to PCR with one of three different sets of primers. Two separate sets of primers were used for the detection of the β1 subunit and one set of primers for rat GAPDH were used as a control. The sequence for the primers used including location (bp) and expected PCR product are shown in Table 1. Primers for GAPDH were run to provide a standard for visual assessment of the amount of cDNA produced during the RT reaction. Primers for GAPDH are show in Table 1. PCR reactions containing primers without cDNA were used as control. The β1 PCR product was confirmed by mapping with the restriction enzymes *Acc*1 and *Pst*1.

sponded to that reported by Isom *et al.* (5). The β1-pAlterXG plasmid (the vector kindly provided by Dr. J. R. Moorman, University of Virginia, Charlottesville, VA) was linearized with *Bam*H1 and used as a template for transcription of cRNA. The cytoplasmic tail of β1 was truncated by the introduction of two stop codons (TGA TGA) at position 190 with the use of PCR to test involvement of the tail in β1-mediated effects. This modification of the β1 subunit caused a truncation immediately after the transmembrane spanning region completely deleting the cytoplasmic tail (βnt). In oocytes coinjected with β1 or βnt, we had no direct method of determining whether β1 was successfully coexpressed with the α subunit in that oocyte. We did, however, assess the quality of the β1 transcript by recording currents from oocytes coinjected with the skeletal muscle α subunit μ1 (μ1 was kindly provided by Dr. Gail Mandel, State University of New York at Stony Brook). If typical effects on μ1 kinetics were observed (i.e., increased decay rate), all oocytes coinjected with that same β1 (or βnt) transcript were analyzed as if the subunit were coexpressed with hH1a.

Methods to determine presence of β1 in rat heart cells. Rat ventricular myocytes were isolated enzymatically as previously described (12). The cells were carefully centrifuged and washed to remove dead cells and debris and yielded healthy appearing cardiac myocytes. Total RNA was isolated according to the procedure of Chomczynski and Sacchi (13). Rat brain total RNA and rat heart total RNA were purchased from ClonTech. RT-PCR experiments were performed with the Perkin-Elmer Cetus GeneAmp RNA PCR kit. Two different sets of primers for the rat β1 were used (Fig. 1; Table 1). Primers to glyceraldehyde-3-phosphate dehydrogenase, a housekeeping gene found in approximately constant levels in rat cells, were used as a control to indicate whether comparable levels of cDNA were present after the RT reaction. The RT reactions contained a final concentration of 5 mM $MgCl_2$, 1 mM each of dNTPs, 1 unit/μl RNase inhibitor, 2.5 μM random hexamers, 2.5 units M-MLV RT, 1× PCR buffer II (Perkin-Elmer Cetus), and 1 μg of total RNA in a total volume of 20 μl. The RT reaction was placed in a Perkin-Elmer Cetus 9600 PCR unit and incubated for 10 min at 22° followed by one program cycle of 15 min at 42°, 5 min at 99°, and 5 min at 5°. A master mix solution with AmpliTaq polymerase (2.5 units final concentration), 10× PCR II buffer (1× final), and $MgCl_2$ (2 mM final) was prepared, and 78 μl was added to each tube after the RT reaction. Appropriate primers were added (0.15 μM final concentration), and the tubes were put through the following cycle: 2 min at 95° 1 min at 95°, and 1 min at 65° for 35 cycles; 7 min at 65° for 1 cycle; and 4° soak. The PCR products were analyzed on a 1.5% agarose gel stained with ethydium bromide. Total RNA samples from rat heart, rat myocytes, and rat brain were used with a primer-only control.

Electrophysiological recordings: whole oocytes. *Xenopus* oocytes were injected with 50–150 ng of cRNA for hH1a alone or in some cases a mixture of cRNA for hH1a and cRNA for β1 or βnt subunits in 3–9-fold excess of that for hH1a (total 50–150 ng). One to seven days after injection, I_{Na} was recorded from cRNA-injected oocytes with a two-electrode voltage-clamp/bath-clamp. A Dagan CA-1 (bath-clamp) with a series resistance compensation circuit (TEV-208, Dagan) was used to make recordings. All recordings were made at 20–22° in a flowing bath solution consisting of 90 mM NaCl, 2.5 mM KCl, 1 mM $CaCl_2$, 1 mM $MgCl_2$, and 5 mM HEPES, pH 7.2. Lidocaine in appropriate amounts was added from a 100 mM stock solution in distilled water. Electrodes contained 3 M KCl and had resistances that ranged from 0.2 to 1.5 MΩ. Data were acquired with the use of pClamp6 software (Axon Instruments) with an Intel-486 based computer. Data were digitized at a 42 kHz and were low pass filtered at 10 kHz (−3 dB).

Voltage control considerations in whole oocytes. The large membrane area of the oocyte (~1-mm-diameter spheres; membrane capacitance >200 nF) prevents the membrane potential from rising sufficiently fast after step changes in the whole-oocyte clamp to accurately study activation and decay of sodium currents. We therefore used macropatch and single-channel patch experiments to study activation and decay, as well as single-channel conductance. Whole-oocyte preparations, however, offer stable recordings of I_{Na} for ≥4 hr, allowing for more-prolonged protocols and study of multiple drug concentrations with wash. For most protocols, peak current was used as an assay to assess sodium channel availability. This measure

TABLE 1
RT-PCR primers for detection of β1 subunit

Primer Sets	Location	Size
		bp
β1 primer set 1		
RATβF1: CGC GGC CCA TGG GGA CGC TGC TGG CTC TCG	Ratβ1 212	
RATβR1: CGG AGC CCA GAG CCA GCG CTA TTC AGC C	Ratβ1 894	682
β1 primer set 1		
RATβF: TAT GAG ATT GAG GTF TTG CAB CTG G	Ratβ1 346	
RATβR: GTA GGC TGG CTC TTC CTT GAG G	Ratβ1 916	580
GADPH primer		
GAPDHF: GAC CCC TCC ATT GAC CTC AAC TAC	127	
GAPDHR: GAT GCC AAA GTT GTC ATG GAT GAC	535	409

MOL PHARM
MOLECULAR PHARMACOLOGY
aspet
Downloaded from molpharm.aspetjournals.org at Zhejiang University on December 1, 2012

MOL PHARM
MOLECULAR PHARMACOLOGY
aspet

appears to be generally less susceptible to errors caused by delayed charging of the membrane. Voltage control problems caused by current flow over series resistance during I_{Na} was not a problem as membrane potential was monitored during most of the experiments and deviations from command were <1 mV.

Electrophysiological recording: patches. Oocytes with >5 μA of peak current were used for macropatch recordings, whereas oocytes with 3–5 μA of peak current were used for single-channel recordings. Macropatch and single-channel I_{Na} were obtained with an E.C.-7 patch-clamp (List-Electronic, Darmstadt-Eberstadt, Germany). The vitelline envelope was removed from the surface of the oocyte immediately before obtaining GΩ seals. This was accomplished by shrinking the oocyte in a hypertonic solution (85 mg/ml of sucrose dissolved in oocyte ringers solution) so the vitelline envelope separated from the membrane. This layer was then easily removed with a pair of fine-tipped forceps. The oocytes were placed into a zeroing bath of 120 mM K^+ aspartate, 20 mM KCl, 1 mM $MgCl_2$, 10 mM EGTA, and 10 M HEPES, pH 7.4. Patch electrodes contained 280 mM Na^+, 1 mM Ca^{2+}, 1 mM Mg^{2+}, 10 mM tetraethylammonium chloride, and 10 mM HEPES, titrated to pH 7.6. Single-channel records were filtered at 3 kHz (−3 dB) and sampled at 12.5 kHz, whereas macropatch currents were filtered at 5 kHz and sampled at 50 kHz. Patch-clamp data were acquired with Axobasic 1.1 as supplied by Dr. Aaron Fox (Department of Pharmacology and Physiology, University of Chicago, Chicago, IL), and analysis was performed with a custom analysis program written and supplied by David Piper (University of Utah). Analogue capacity compensation was achieved with the circuitry of the E.C.-7, and any remaining capacitance was compensated via the P/4 method of Bezanilla and Armstrong (14). All experiments were performed at room temperature (20–22°).

Experimental protocols and analysis. Details of the voltage protocols are provided with the data. Standard holding potential for whole-oocyte clamp was −120 mV and for patch was −130 mV. The frequency of stimulation within a protocol was carefully considered and tested so that no effects of a previous stimulation would be present in a subsequent test. For the development protocols, we inserted test steps without a conditioning step at the beginning, middle, and end of the protocol to ensure that no accumulation of inactivation or unrecovered drug block had occurred. For recovery protocols, we inverted the order of the recovery times to ensure that the order did not influence the recovery time course. Peak currents were measured as the maximum negative current after the depolarization. Leak correction was unnecessary because the expressed currents in the range studied were always more than 20-fold the amplitude of endogenous oocyte currents. Residual outward capacity current at the time of peak current caused an underestimation of peak I_{Na} for uncorrected traces. The amount of this underestimation was measured from the steady state inactivation protocol with a 2-msec clamp back for which all I_{Na} were inactivated and used to correct peak currents to the standard test protocol of −10 mV. Data were fit to model equations using nonlinear regression (Procedure NLIN) with the use of SAS Institute (Cary, NC) statistical software running on a SUN ELC workstation. Parameter estimates are given ± the standard error for the parameter estimate. For the exponential fits for recovery and decay, the data were also fit to a one-component model, and an F ratio ($p < .05$) was used to determine whether the two-component fit was better than the one-component fit. Mean data are reported with their standard deviation. All determinations of statistical significance of mean data were performed with Student's t test for comparisons of two mean values or by one-way ANOVA followed by Bonferroni's t test for comparison of more than two mean values.

Results

The β1 subunit in heart cells. An important issue in studying the effects of association β1 with the heart α subunit is whether β1 is present in the same cells in heart as the

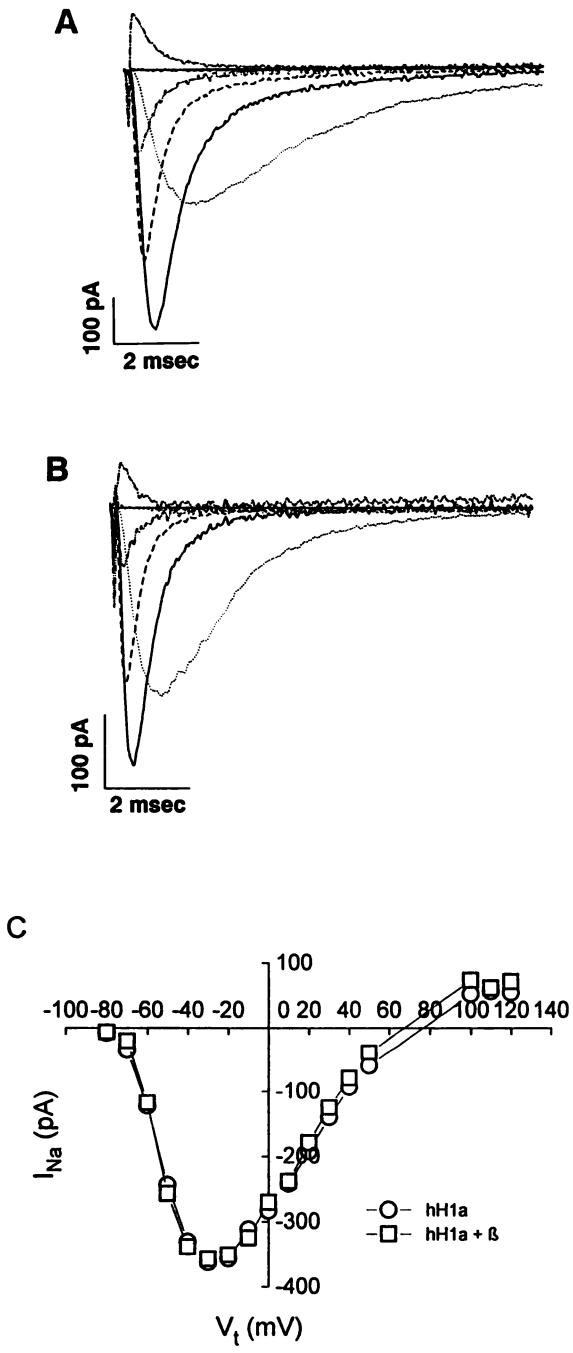

Fig. 2. β1 subunit had no effect on I_{Na} time course in macropatches. A, I_{Na} resulting from coexpression of β1 with hH1a. Families of oocyte-attached macropatch currents are shown for step depolarizations from −130 mV to the test potentials (V_t) indicated. B, I_{Na} resulting from expression of hH1a alone, with the same protocol as in A. C, Peak current-voltage relationship for I_{Na} in macropatches, with the same oocytes as in A and B.

α subunit. The presence of β1 in mRNA isolated from total heart has been demonstrated (2), including the cloning of human β1 from a heart cDNA library (3). It may be, however, that mRNA found in these total heart preparations came from nerve or other noncardiac cells. To address this issue, we isolated myocytes from rat ventricle and demonstrated the presence of mRNA for the β1 subunit in the same cells where the α subunit is also located (Fig. 1). These experiments show that β1 mRNA can be detected in myocytes,

Downloaded from molpharm.aspetjournals.org at Zhejiang University on December 1, 2012

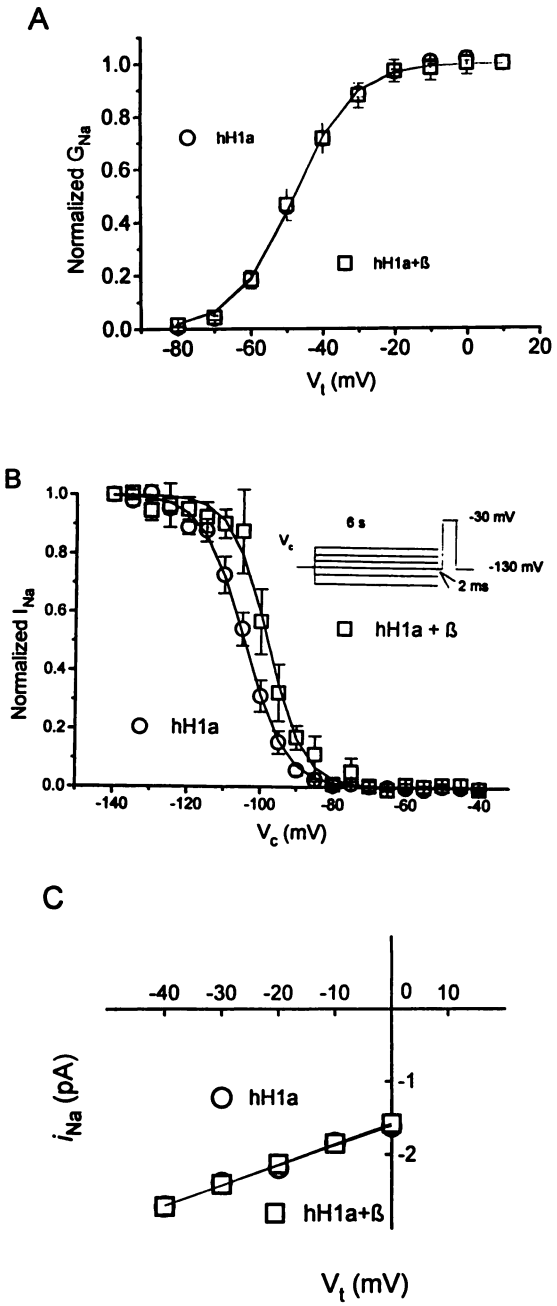

Fig. 3. β1 subunit affected inactivation but not activation or single-channel conductance. A, Voltage-activation relationships are shown as mean normalized chord conductances ($G_{Na} = I_{Na}/(V_t - V_r$; where V_r is the reversal potential) from data obtained as in Fig. 1. Data shown are mean values for eight (hH1a) and five (hH1a+β) experiments in different oocytes. *Solid lines*, fits to the Boltzmann distribution: $G_{Na} = 1/[1 + \exp(V_{½} - V_t)/k]$ where k = 8.1 and $V_{½}$ = −47.9 mV for hH1a and k = 8.3 and $V_{½}$ = −48.1 for hH1a+β. B, Coexpression of β1 with hH1a caused a depolarizing shift in steady state availability. *Inset*, two-pulse steady state availability protocol; the 6-sec conditioning step (V_c) ranged from −140 to −30 mV in 5-mV increments. Peak I_{Na} were measured for the second test step to −30 mV and normalized to the I_{Na} for V_c = −140 mV. Mean normalized peak I_{Na} (*Normalized INa*) are shown for hH1a alone (seven experiments) and for hH1a+β (five experiments). *Lines*, fits to a Boltzmann distribution: $G_{Na} = 1/[1 + \exp(V_C - V_{½})/k]$ where k = 5.6 and $V_{½}$ = −104 mV for hH1a and k = 5.0 and $V_{½}$ = −98 mV for hH1a+β. C, Coexpression of β1 did not affect the single-channel conductance of hH1a. Unitary current amplitudes (i_{Na}) were determined with the variance mean analysis method of Patlak (23) using a half-amplitude threshold cutoff for five patches with hH1a and five patches with hH1a+β. Single-channel conductances were calculated from the slope of the current-voltage relationship in 280 mM Na^+. For hH1a, single-channel conductance was 27 pS; for hH1a+β, single-channel conductance was 28 pS. *Vertical bars*, standard errors. Error-bars smaller than the symbols are not shown.

although nothing can be deduced regarding the relative amount of mRNA found in myocytes compared with total heart, nor can trace contamination from noncardiac cells carried over during myocyte isolation be completely ruled out. Nevertheless, these results are the most suggestive data that β1 mRNA and, presumably, β1 protein are found in cells that also express the rat heart α subunit.

In macropatches, β1 shifted inactivation but did not affect activation or decay. Activation and decay kinetics for a step depolarization are very sensitive to the rise time of the clamp. We therefore studied these properties in on-cell macropatches containing multiple (usually >100) channels where the small membrane capacity in the patch could be rapidly charged. Families of macropatch currents for hH1a alone (Fig. 2A) and for hH1a coexpressed with the rat brain isoform of the β1 subunit (hH1a+β, Fig. 2B) showed no obvious differences in the time course of the macroscopic currents. A plot of the peak sodium current (I_{Na})-voltage relationships (Fig. 2C) showed that both hH1a and hH1a+β activate at ~−70 mV and peak at ~−30 mV. Summary data for peak currents in response to step depolarizations analyzed as activation curves (Fig. 3A) confirmed no differences in activation kinetics with and without coexpression of β1. The voltage dependence of steady state availability (also called inactivation or h_∞) was studied using a 6-sec conditioning step. β1 caused an ~6-mV positive shift in the midpoint (Fig. 3B) of this relationship. Finally, β_1 had no effect on single-channel conductance (Fig. 3C), which was ~28 pS in both cases.

Macroscopic current decay is not affected by β1. Macroscopic current decays in macropatches were always better fit by the sum of two exponential components, one slow (τ_s) and one fast (τ_f), both with and without coexpression of β1. A plot of the voltage dependence of the time constants of the fast components (Fig. 4A) indicates no difference for the rapid component. The amplitude of the slow component was only 1–5% of the total decay, and there also was no difference in τ_s with and without coexpression of β1 (data not shown).

Compared with the macropatch, the whole-oocyte clamp is more subject to clamp errors caused by slow membrane charging (see Experimental protocols and analysis). It does, however, allow for more prolonged and stable recordings of I_{Na} than does the macropatch technique. The whole-oocyte clamp was used in the remainder of the study to study longer voltage-clamp and solution change protocols than could be achieved with the macropatch clamp. In whole oocytes, macroscopic current decay was assessed by the time it took for the current to decay to half the peak amplitude ($t_{½}$, Fig. 4B). Analysis of three oocytes with hH1a and three oocytes with hH1a+β chosen to have comparable maximal peak currents at 3–4 μA confirmed the macropatch results that β1 had no significant effect on I_{Na} decay kinetics from a holding potential of −120 mV. Fig. 5A (*insets*) shows representative current traces in response to depolarizations from different conditioning potentials (V_c) for oocytes with hH1a alone or for hH1a+β. β1 had no effect on decay rate with different V_c values. In addition, current traces with different amplitudes

Downloaded from molpharm.aspetjournals.org at Zhejiang University on December 1, 2012

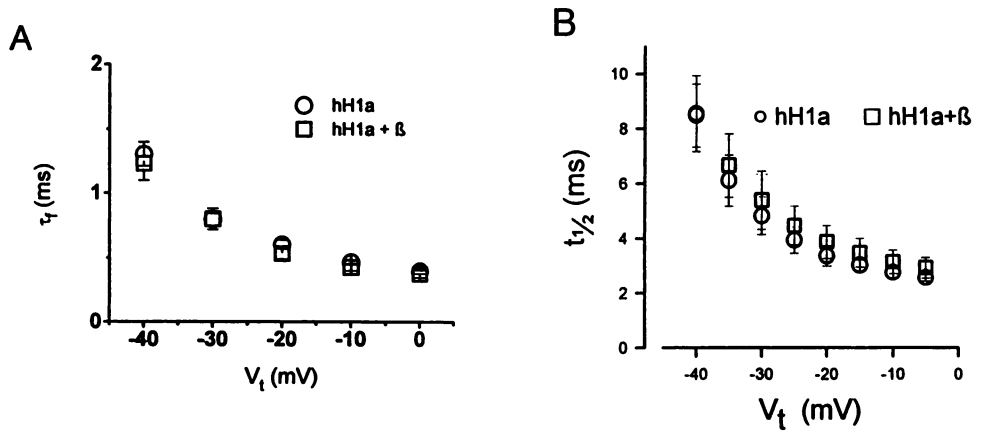

Fig. 4. β1 did not affect I_{Na} decay for hH1a in macropatches and whole oocytes. A, Mean data for the major fast component (τ_f) of decay are plotted for the test depolarization V_t used to elicit I_{Na}. The portions of the I_{Na} traces beginning 40 μsec after peak I_{Na} were fit to a sum of exponentials: $I_{Na}(t) = [A_f * \exp(-t/\tau_f)] + [A_s * \exp(-t/\tau_s)]$, where A_f and A_s represent the amplitudes of the fast and slow components respectively; τ_f and τ_s represent the time constants of the fast and slow components; and t represents time. The program used was Discrete (24), which determines whether one or more components better fit the data. Two components better fit the data between −40 and 0 mV. The fast decay component always dominated, comprising between 95% and 99% of the total amplitude. B, In whole oocytes, β1 did not affect the time for peak current to decay to half-amplitude ($t_{½}$). $t_{½}$ was measured as the time it took I_{Na} to decay to 50% of peak amplitude.

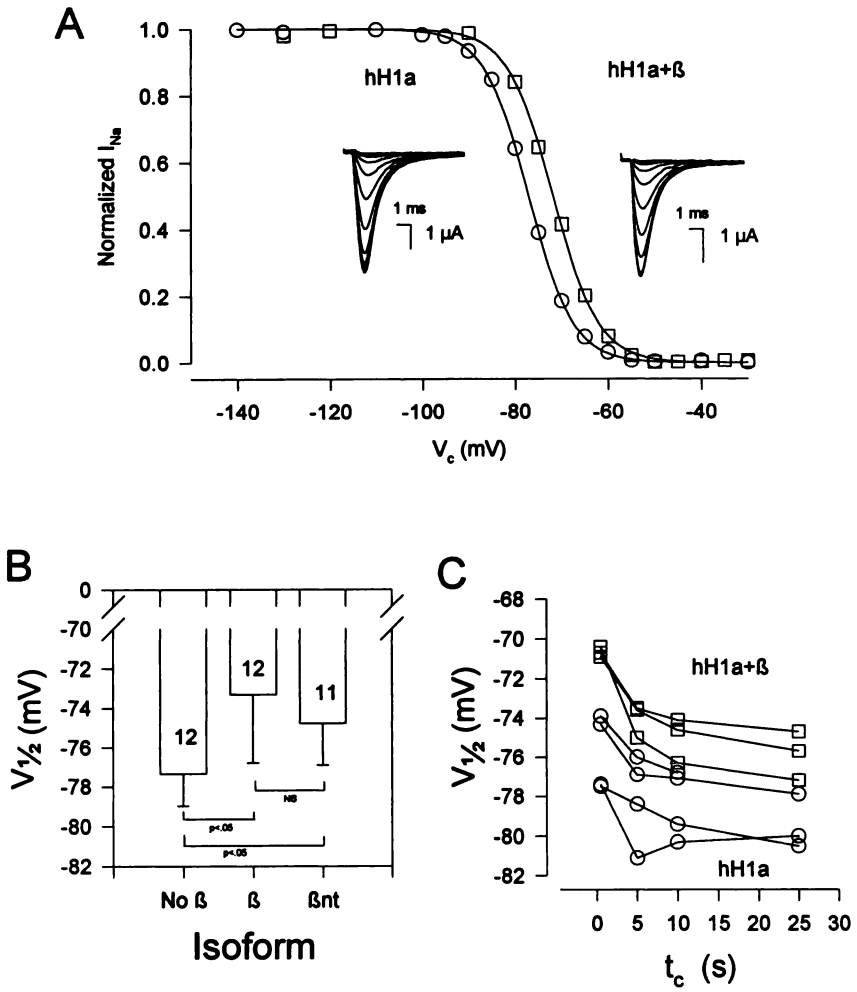

Fig. 5. β1 shifted steady state inactivation in whole oocytes. A, Examples of steady state inactivation relationships (see *protocol diagram inset*, t_c = 25 sec) with and without coexpression of the β1 subunit. *Insets*, capacity-corrected current traces in response to the test step for the different conditioning potentials (V_c). Peak I_{Na} were fit to a Boltzmann equation: Peak $I_{Na} = I_{Na\text{-}max}[1 + \exp(V_c - V_{½})/\text{slope}]^{-1}$ where $I_{Na\text{-}max}$ is the predicted maximum peak I_{Na}, and $V_{½}$ and slope are the midpoint and slope, respectively, of the Boltzmann relationship. *Solid lines*, fits of non-normalized data to the Boltzmann equation that were later normalized by dividing by the fitted parameter $I_{Na\text{-}max}$. For plotting data, peak I_{Na} versus V_c peak currents were normalized to the largest peak obtained. The parameters of the fits for these examples with and without β, respectively, were −71.8 and −77.1 mV for $V_{½}$, 4.89 and 4.79 for the slope factor, and 3.38 and 4.93 μA for $I_{Na\text{-}max}$. B, Summary data for $V_{½}$ of steady state inactivation with and without β1 and with the cytoplasmic tail deletion mutant β βnt. The conditioning potential duration was 10 sec. *Bars*, mean data for the numbers of experiments indicated in the bars. *Vertical lines*, standard deviations. β1 and βnt subunits were associated with a depolarizing shift in $V_{½}$ without a significant effect on slope *k*. Experimental numbers are shown within the bars. One-way ANOVA indicated a significant difference in mean values (F = 7.69, $p < .001$) and p values from the Bonferroni t test comparison for difference of the means are indicated. The t statistic for no β versus β was 3.894, for no β versus βnt was 3.300, and for β versus βnt was 1.367. C, Steady state inactivation protocols with conditioning durations t_c of 0.5, 5, 10, and 25 sec were performed in three oocytes with β1 and four oocytes without β1 to characterize how long it takes to reach steady state. The plot shows that $V_{½}$ shifts in a negative direction for t_c <10 sec but is nearly stable between 10 and 25 sec.

peak at the same time, an indirect but sensitive index of voltage control during flow of I_{Na}.

β1 shifted steady state inactivation in whole oocytes. The effect of β1 on steady state inactivation was assessed by measuring peak currents elicited after a 25-sec V_c. Examples for oocytes with hH1a alone and for hH1a+β are shown in Fig. 5A. A Boltzmann fit to a plot of the peak currents shows that the midpoint $V_{½}$ was shifted 5.3 mV in the positive direction by coexpression with β1. Summary data (Fig. 5B) show that β1 caused a statistically significant 3.9 mV posi-

MOL PHARM
MOLECULAR PHARMACOLOGY
aspet
Downloaded from molpharm.aspetjournals.org at Zhejiang University on December 1, 2012

MOL PHARM

MOLECULAR PHARMACOLOGY

tive shift in mean $V_{½}$. β1 mutants with deleted cytoplasmic tails (βnt) also showed a shift. Steady state is depicted in quotation marks because it is often assumed that the t_c) is sufficiently long to achieve a steady state distribution between the rested and inactivated states, but this is rarely tested. The data in Fig. 5A are for t_c of 25 sec; for Fig. 4B, the data are for t_c of 10 sec. We elected to show data for these relatively long conditioning potentials because of results such as those obtained in Fig. 4C where $V_{½}$ results are shown for t_c of 0.5–25 sec in three oocytes with hH1a+β and in four oocytes with hH1a alone. Steady state would be indicated by no change in $V_{½}$ with prolonging t_c. Although a true steady state may never be reached, even for long t_c, $V_{½}$ changed by several millivolts when t_c was increased from 0.5 sec to 5 sec but <1 mV for an increase from 10 sec to 25 sec. This indicated that at least a near steady state was achieved with a 10-sec t_c. The $V_{½}$ values for hH1a+β were more positive for all of the t_c tested, but we did not test t_c of <500 msec.

Lidocaine shifted voltage dependence of $V_{½}$ and provided an estimate of state-dependent binding for hH1a and hH1a+β. Lidocaine is known to exhibit state-dependent binding with different affinities for the resting and the inactivated states of the channel (15, 16; Fig. 6, *inset*). A greater affinity of lidocaine for the inactivated state causes use-dependent or phasic block, and it also causes a negative shift in the midpoint of the inactivation relationship. In experiments and analysis that parallel those of Cohen *et al.* (17), we measured the concentration dependence for the lidocaine shift of $V_{½}$ for oocytes with hH1a+β and hH1a alone (Fig. 6). We first verified that lidocaine interaction with the channel at each dose reached a steady state during t_c (defined arbitrarily as <1 mV change in $V_{½}$ for the next increment in t_c as in Fig. 5C). For lidocaine concentrations of <10 μM, this required t_c of 25 sec. Dissociation constants for the inactivated state K_{di} and for the resting state K_{dr} were calculated according to Bean *et al.* (17) (see Fig. 6 for the equation and Table 2 for the results of the fit). K_{di} was not affected by coexpression with β1, but K_{dr} was predicted to be increased by β1. The confidence intervals for estimates of K_{dr}, however, were wide (see Fig. 6 legend). Lidocaine interaction rates with the resting state and with the inactivated state were then measured by more direct and model-independent methods.

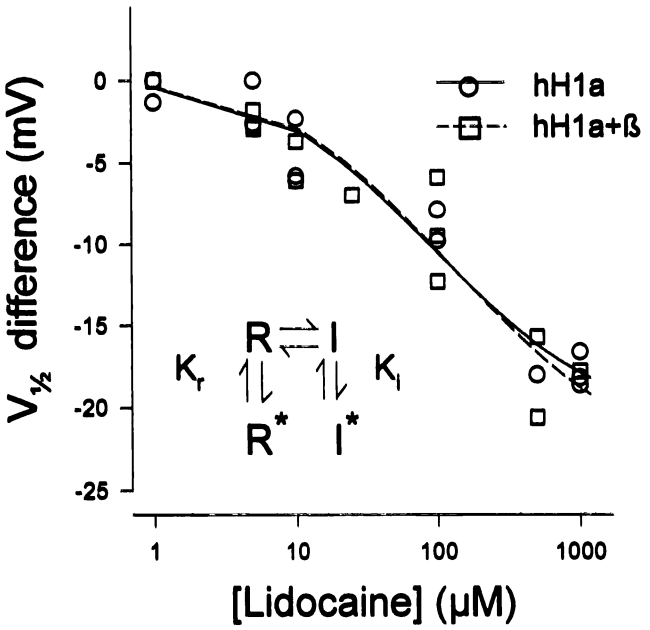

Fig. 6. β1 did not affect the lidocaine-induced shift in the voltage dependence of sodium channel availability. This protocol was intended to assess affinity of lidocaine for the inactivated state. Steady state inactivation relationships (with t_c = 10 or 25 sec) were fit to a Boltzmann equation, and the midpoint ($V_{½}$) and Boltzmann slope were determined as for Fig. 3. Lidocaine had little effect on slope, but it consistently shifted the $V_{½}$ in the negative direction. The difference in the $V_{½}$ between control and lidocaine is plotted against lidocaine concentration. The data are individual data points (14 experiments in 9 oocytes for hH1a and 13 experiments in 10 oocytes for hH1a+β1). *Lines*, fits to the data to the equation: $V_{½}$ difference = 5 * log(1 + [lidocaine]/K_{dr})/(1 + [lidocaine]/K_{di}) where K_{dr} is the affinity constant for the resting state of the channel, K_{di} is the affinity for the inactivated state of the channel, and 5 is the mean Boltzmann slope. For cells without β1, K_{di} = 12 ± 3 μM and K_{dr} = 727 ± 442 μM; for oocytes with β, K_{di} = 13 ± 4 μM and K_{dr} = 1206 ± 1409 μM.

β1 decreased resting lidocaine block. Resting or tonic block was measured by comparing the peak current in lidocaine with the peak current in control solutions for a depolarization from −120 mV to −10 mV after a prolonged (>2-min) duration at the holding potential. Dose-response curves (Fig. 7) for hH1a alone and with wild-type β1 and the tail deletion mutant βnt show that both β forms caused a 2–3-fold decrease in affinity (see Fig. 6 legend and Table 2) to nearly the same extent as that predicted by the $V_{½}$ shift.

β1 increased recovery from lidocaine block. Recovery from inactivation in control and from lidocaine block was studied by identical two-pulse protocols (Fig. 8A, *inset*). In control, recovery from inactivation was best fit by two exponentials, but the majority of the recovery (>80%) was in the rapid component. Summary data for recovery parameters at recovery potentials of −130, −120, −110, and −100 mV in control for hH1a, hH1a+β, and hH1a+βnt showed no significant difference in the rapid time course of recovery (Fig. 8B). When recovery was studied in the presence of 100 μM lidocaine, the recovery time course could be described by a single exponential and the τ was twice as slow for hH1a alone compared with that for hH1a+β (Fig. 8A). For ≥100 μM lidocaine, the recovery time constant was not concentration dependent (data not shown). This suggests that for these higher concentrations, all channels were blocked by lidocaine and recover with the slow time constant characteristic of drug dissociation at −120 mV, presumably from the resting state. Fig. 8C shows summary data for recovery from lidocaine block for hH1a alone, hH1a+β, and hH1a with the tail deletion β mutant βnt. The data show that both β1 and βnt double recovery from lidocaine block (τ decreased from ≅800 msec to ≅400 msec).

β1 did not affect inactivated-state lidocaine block. Development of block was studied by a two-pulse protocol (Fig. 9A, *inset*). A variable-duration conditioning pulse to −20 mV was followed by a 100-msec recovery period, after which a test depolarization was used to assay channel availability. In control solutions, the 100-msec recovery interval at −120 mV was sufficient to allow recovery from inactivation for all except the longest conditioning durations. For long conditioning durations, an increasing proportion of channels recover with a slow time constant (~500 msec). The effects of slow recovery to decrease peak I_{Na} are apparent for conditioning durations of >1 sec and increase to 8.2 sec. β1 did not affect slow recovery in this example (Fig. 9A), and mean

Downloaded from molpharm.aspetjournals.org at Zhejiang University on December 1, 2012

aspet

TABLE 2
Lidocaine interaction with resting (r) or inactivated (i) state

Parameter	Protocol	Rate value (hH1a)	Rate value (hH1a+β)
	Tonic block	534	1342
K_{dr} (μM)	SSI shift	727	1206
k_r ([μM^{-1}msec^{-1}] 10^{-6})	Calculated	2.6	1.9
I_r (msec^{-1})	Recovery	0.0014	0.0026
	Dev. amp.	8.8	11.6
K_{di} (μM)	Dev. (τ)	4.4	4.6
	SSI shift	11.7	12.5
k_i ([μM^{-1}msec^{-1}] 10^{-6})	Dev. (τ)	43.2	42.3
I_i (ms^{-1})	Dev. (τ)	0.0019	0.0020

K_{dr}, dissociation constant for the resting state; k_r, on rate to the resting state; I_r, off rate from the resting state; K_{di}, dissociation constant for the inactivated state; k_i, on rate to the inactivated state; i_r, off rate from the inactivated state.
Protocols refers to the method used to obtain the values. Tonic block is as in Fig. 7 legend; SSI shift is as in Fig. 6 legend; Calculated is according to $k_r = K_{dr}/I_r$; Dev. Amp is from fits to amplitudes of development as in Fig. 9B legend; and Dev. (τ) is from fits to time constant of development as in Fig. 9C legend.

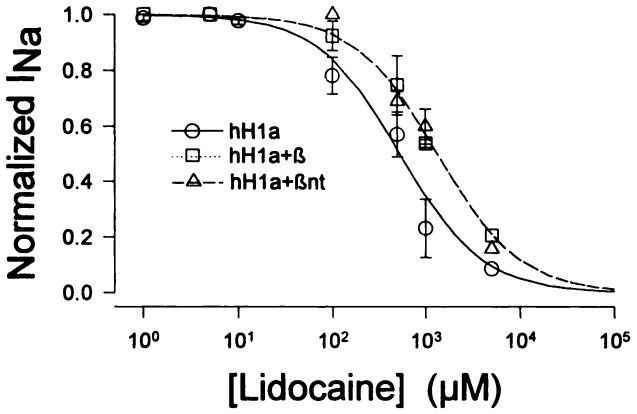

Fig. 7. β1 decreased tonic block by lidocaine. The proportion of I_{Na} remaining in the presence of lidocaine was determined by dividing the peak I_{Na} for different concentrations of lidocaine by the peak I_{Na} in control solutions in response to a step depolarization from −120 mV to −10 mV. *Symbols with standard error bars*, mean from two to six measurements; *symbols without error bars*, single data points. *Lines* represent fits to a single-site binding equation: Normalized I_{Na} = 1/(1 + [lidocaine]/K_d) where K_d is the half-blocking dose. The half-blocking doses ± asymptotic standard deviation of the parameter estimates were 534 ± 95 μM (19 doses from 13 oocytes) without β1, 1342 ± 181 μM (16 doses from 14 oocytes) with β1, and 1347 ± 186 μM (12 doses from 9 oocytes) with βnt.

summary data for the fractional decrease in I_{Na} in control for an 8.2-sec conditioning duration were 0.69 ± 0.12 (8 experiments) for hH1a alone and 0.74 ± 0.07 (11 experiments) for hH1a+β. In the presence of 10 μM lidocaine, a greater fractional decrease in current (relative to control) was found (Fig. 9A), presumably caused by lidocaine binding to the inactivated state during the preceding conditioning depolarization. For these results to indicate inactivated-state binding, several assumptions must be examined. The 100-msec recovery interval was designed and assumed to allow for recovery from inactivation of unblocked channels but to not allow recovery of lidocaine-blocked channels. To the extent that these assumptions are true, the peak I_{Na} in the second depolarization represents the number of channels blocked by lidocaine during the inactivated step. Lidocaine recovery occurs with a time constant of ~400 msec (without β1) and ~800 msec (with β1) at −120 mV; therefore, ~22% and ~12%, respectively, of blocked sodium channels will recover in 100 msec, which means that peak I_{Na} underestimates the block because of this error. Rapid recovery from inactivation of unblocked channels is ~10 msec; therefore, rapid recovery was nearly complete in 100 msec. A proportion of current, ~0.15 for 1-sec conditioning duration and increasing for longer conditioning durations, recovered with a time constant of ~500 msec. Thus, for the longer conditioning durations, slow recovery will cause an overestimate of lidocaine block. These two errors at least partially offset in a way that depends on conditioning duration. We analyzed data correcting for both of these known errors (analysis not shown) and found only minor differences that did not affect the conclusions. We therefore present summary data for the amplitude of block Fig. 9B and for the time constant of development (τ, Fig. 9C) from the uncorrected analysis. The dissociation rate for the inactivated state was estimated simply by fitting a single-site binding curve to the amplitude of the block. The association rate and dissociation rate were estimated separately from the τ of development, and the results are given in Table 2. β1 caused no discernible differences in the interaction of lidocaine with the inactivated state by any of the three methods used (Figs. 6, 9B, or 9C).

β1 decreased use-dependent lidocaine block. Use-dependent, or phasic, block refers to the additional lidocaine block developed when the membrane is repetitively depolarized. A more rapid recovery from the lidocaine-bound resting state with β1 present predicts that there will be less block in response to a train of depolarizations with β1 because of greater recovery in the interval between depolarizations. Additional fractional block was measured by subtracting the peak current for the last depolarization in the train from that for the first block in the train and dividing by the peak current for the first depolarization. For depolarizations from −120 mV to −10 mV lasting 20 msec with 80 msec between depolarizations (10 Hz), a steady state peak current was reached within 50 pulses. In 100 μM lidocaine, the block was 0.61 ± 0.07 for hH1a alone and 0.28 ± 0.19 for hH1a+β (five experiments).

Discussion

Comparison with previous results: kinetics. The β1 subunit has large effects on inactivation kinetics for brain and skeletal muscle sodium channel α subunits expressed in oocytes. Coexpression of β1 accelerates the macroscopic decay of I_{Na} severalfold and for short (<500-msec) conditioning durations shifts the steady state voltage-dependent availability in the negative direction by as much as 20 mV (5, 6; for reviews, see Refs. 18 and 1). Both of these effects tend to make the kinetics more closely resemble those found in native tissues. Unlike brain and skeletal muscle sodium chan-

MOL PHARM
MOLECULAR PHARMACOLOGY
aspet
Downloaded from molpharm.aspetjournals.org at Zhejiang University on December 1, 2012

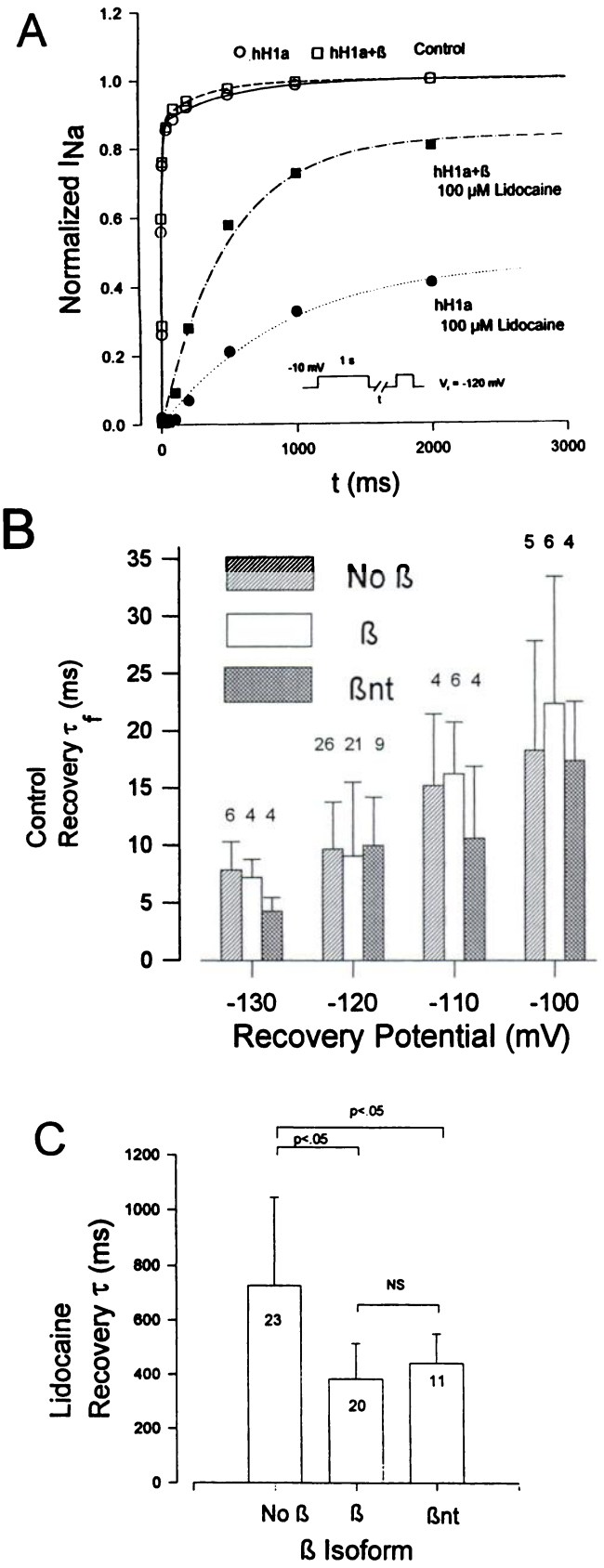

Fig. 8. β1 had a small effect on recovery from inactivation and greatly accelerated recovery from lidocaine block. A, Recovery time course (see *protocol inset*) without β1 and with β1. The I_{Na} for the data and for the fits were normalized for the maximum current in control for each oocyte. In control, the *lines* are two component exponential fits with τ_f = 11 msec and τ_s = 484 msec without β1 and τ_f = 10 msec and τ_s = 306 msec with β with a relative contribution of the amplitudes of the slow components of 0.13 at V_r = −120 mV. B, β1 and the β1 mutant βnt had no significant effect on recovery from inactivation. Mean data with standard deviations for the fast recovery time constant (τ_f) are plotted for oocytes expressing hH1a without β1 (*No β*), hH1a with β1 (*β*), and for hH1a with β1 mutated to remove the cytoplasmic tail (*βnt*) are shown for four different recovery potentials. ANOVA analysis indicated no significant differences among the mean values for τ_f without β1, with β1, and with βnt. Experimental numbers are shown above the bars. C, Summary data for recovery time constants in lidocaine without β1 and with β1 and βnt. *Bars with vertical lines*, mean data representing standard deviations; *numbers in the bars*, number of experiments. Data are for lidocaine concentrations from 100 μM to 1000 μM. ANOVA indicated significant differences in the mean values (F = 13.5, p < .001), and Bonferroni's t test indicated that β1 and βnt were equally-effective in increasing recovery from lidocaine block.

nel α subunits, however, cardiac sodium channel α subunits expressed alone in oocytes produce currents that closely resemble those in native tissues (7). Makita *et al.* (3) coexpressed a human β1 with hH1 in oocytes and found no effect on macroscopic decay rates for a depolarization from −120 mV to −20 mV, no effect on steady state inactivation for a conditioning potential of 200-msec duration (midpoint ~−68 mV), and no effect on recovery at −120 mV. More recently, Nuss *et al.* (8) found that coexpression of β1 with hH1 accelerated both decay and recovery, but a small shift in steady state availability was not statistically significant. Our more detailed studies of decay, including macropatch experiments, found that coexpression of β1 with hH1a had little or no effect on decay over a wider voltage range of depolarizations. Our studies on recovery over a wider range of recovery potentials also demonstrated no detectable effects. Unlike previous studies, we detected a consistent and statistically significant positive shift of several millivolts in the midpoint of the steady state inactivation relationship with hH1a+β. We also found for both hH1a and hH1a+β that the midpoint of the relationship shifted 3–4 mV in the negative direction when the conditioning durations in the steady state inactivation protocol were increased from 500 msec to 5 sec, but it shifted <1 mV between 5 and 10 sec and between 10 and 25 sec (Fig. 5C). Studies with shorter conditioning durations, such as those used by Makita *et al.* (3) and Nuss *et al.* (8), are farther from steady state and will yield less negative midpoints and perhaps obscure the shifts we have observed with longer conditioning durations. Although the shifts are only several millivolts, they could be physiologically or pathologically important if, for example, the cell is operating at a resting potential on the steep slope of the voltage-dependent availability relationship. Many of our results for β1 effects on kinetics are negative and agree with the results of Makita *et al.* (3) rather than with those of Nuss *et al.* (8). The reasons for these differences are not clear, but elicitation of kinetic effects can be quite dependent on the specific protocols used to elicit the effects, and we cannot exclude the possibility that protocols done with, for example, more depolarized holding and recovery potentials might elicit different β1 effects on kinetics. Other considerations include minor differences in the structures of α and β1 subunits used and possible differences in efficiency of expression of β1. Overall, however, and based on our experiments with lidocaine, we agree with the major conclusion of Nuss *et al.* (8) that β1 can affect cardiac α subunit function.

MOL PHARM
MOLECULAR PHARMACOLOGY
aspet
Downloaded from molpharm.aspetjournals.org at Zhejiang University on December 1, 2012

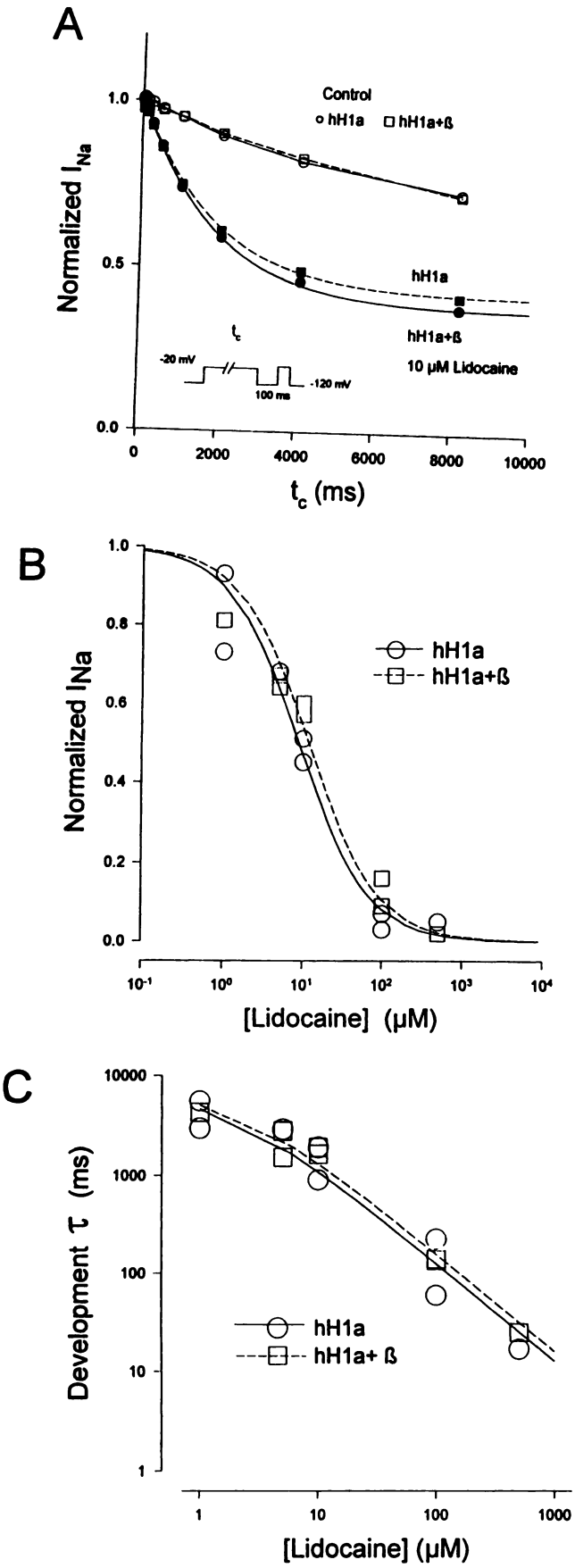

Fig. 9. β1 had little effect on inactivated state block by lidocaine. A, Development of lidocaine block to the inactivated state was assessed

Comparison with previous results: lidocaine block. Block of sodium channels by local anesthetics such as lidocaine has a complex dependence on how the block is produced and measured. Lidocaine block can be categorized into nonphasic block, also called rest or tonic block, and phasic block, also called extra block, use-dependent block, frequency-dependent block, or state-dependent block. Phasic block is usually explained in terms of the modulated-receptor model (15, 16) as enhanced binding of the drug to one or more of the kinetic states of the channel. In the context of this model (Fig. 6), tonic block by lidocaine is caused by binding to the resting state of the channel with one affinity, and phasic block is caused by higher affinity binding to the inactivated state. Rest block can be estimated relatively simply by measurement of the effect of lidocaine on the amount of current elicited for a depolarization after a prolonged rest at very negative potentials when all channels should be in the resting state. Inactivated state block can be measured in several ways (see Figs. 6 and 9). We estimated apparent interaction rates for lidocaine with the resting state and the inactivated states for hH1a alone and hH1a+β by a number of independent methods and obtained consistent results (Table 2). The largest effect of coexpression of β1 with hH1a is to increase the half-blocking concentration for lidocaine at rest (K_{dr}) from ~500 µM to 1400 µM without affecting the half-blocking concentration (K_{di}) for the inactivated state, which was ~10 µM. Our results suggest that most of the difference in affinities can be accounted for by the faster recovery rate for hH1a+β (Table 2). For native sodium channels in rabbit Purkinje fibers, Bean *et al.* (17) found a resting affinity of 440 µM and an inactivated affinity of 10 µM. In a voltage-clamp study in single cells, Starmer *et al.* (19) estimated an inactivated affinity of 19 µM. For human cardiac sodium channels expressed in oocytes without β1, Chahine *et al.* (20) found the half-block at −100 mV to be 226 µM and the K_{di} of 11 µM and K_{dr} of 3.9 mM when fit to the shift in the availability midpoint (similar to Fig. 6). Krafte *et al.* (21) found a resting affinity of 521 µM at −100 mV for hH1 alone in oocytes. Considering different conditions and protocols, our results without β1 are similar to those reported previously for human heart chan-

for a variable length depolarization t (see *protocol inset*). In this protocol, lidocaine was assumed to bind during the variable length conditioning depolarization, and the second test depolarization was assumed to represent the amount of lidocaine block developed during the first depolarization. See text for a discussion of these assumptions. Peak I_{Na} for the second depolarization were normalized to the peak I_{Na} without a conditioning depolarization. Lidocaine caused a more rapid and greater fall in peak I_{Na} than in control, and this decline was best fit by a single exponential fit (*lines*). In these examples without β, τ = 1913 and amplitude = 0.60, and with β, τ = 1914 and amplitude = 0.58. B, Concentration response for the amplitude of inactivated state block. Fractional I_{Na} was computed by dividing the peak current in lidocaine by the peak current in control for an 8.2-sec conditioning depolarization. *Lines* are fits to a single-site binding equation: Normalized I_{Na} = $1/(1 + [\text{lidocaine}]/K_{di})$ where K_{di} is the half-blocking dose. The half-blocking doses ± asymptotic standard deviation of the parameter estimates and total number of data points were 8.8 ± 1.4 µM (eight experiments) without β1 and 11.6 ± 1.4 µM (eight experiments) with β1. C, Affinity for inactivated state estimated from the time constant (τ) of development of block. The concentration dependence of the τ for development of lidocaine block in response to the two-pulse protocol (A, *inset*) is shown for oocytes without β1 and with β1. *Lines*, fits to the equation: $\tau = 1/(l_i + k_i[\text{lidocaine}])$ where l_i is the off rate for the inactivated state and k_i is the on rate to the inactivated state. The parameter fits are reported in Table 2.

MOL PHARM
MOLECULAR PHARMACOLOGY
aspet
Downloaded from molpharm.aspetjournals.org at Zhejiang University on December 1, 2012

nels expressed without β1 in oocytes and to those reported for native channels. Our results for lidocaine rest block without β1 appear to be closer to those of native channels, suggesting that native adult cardiac channels *in vitro* do not show a β1 effect. Lidocaine block, however, is exquisitely sensitive to the measurement protocols, including holding potential, temperature, pH, and the ionic environment. Also, it is not known whether lidocaine action in channels expressed in oocytes differs from that when the channels are expressed in mammalian cells. Thus, it would be wrong to conclude from these data that β1 effect is not present in adult heart.

Mechanism of β1 effects on kinetics and lidocaine block. Sites responsible for both inactivation and lidocaine block are thought to reside in the pore on the cytoplasmic side of the channel (for review, see Ref. 22). β1 is predicted to have a single transmembrane spanning segment with a long cytoplasmic tail (5). A plausible hypothesis for the mechanism of β1 action would be a direct interaction of the β1 tail with the structures responsible for inactivation and lidocaine block. Our results, however, show that the β1 cytoplasmic tail was not necessary to accelerate recovery and decrease lidocaine block. The complex state and voltage dependence of lidocaine block of the sodium channel allow for changes in block by at least three not necessarily mutually exclusive general mechanisms: (i) the affinity at the binding site can be altered, (ii) access or egress of the lidocaine to or from the binding site can be altered, and (iii) binding can be altered by changing gating kinetics (i.e., by altering dwell time in higher/lower affinity states). A minimal effect on kinetics mitigates against the third mechanism, and a lack of effect of the tail mitigates against a direct effect of the tail to alter affinity or augment egress. Our results favor an indirect effect of the transmembrane or extracellular domain of β1 altering α subunit structure to either decrease affinity for the resting state at the binding site(s) or to augment egress.

Limitations and caveats. Despite taking the measures described in Materials and Methods, undetected failure to coexpress β1 might tend to obscure or minimize β1 effects in our study as well as in previous studies, which means that we may have underestimated β1 effects. Also, we used transcript for rat brain β1 rather than human. The β1 subunit shows no tissue dependence and very little species-dependent sequence differences, but such differences cannot be discounted entirely in interpreting these results. Limitations from issues regarding voltage control must also be considered, and these have been addressed. Finally, although the effects we report might be interpreted as being caused by a specific β1 association with the α subunit of hH1a, the results do not prove such an association because β1 could conceivably affect function by, for example, channel processing or regulation.

Summary. Coexpression of β1 subunits is capable of altering the function of the human cardiac sodium channel α subunits in oocytes. The most dramatic effect is acceleration of recovery from lidocaine block, and experiments with β1 mutants indicate that the cytoplasmic tail is not responsible for this effect. Inactivation recovery kinetics at the same potential where lidocaine recovery is affected suggests that this effect is caused by an allosteric change at the lidocaine binding site, but an action through subtle effects on inactivation kinetics cannot be excluded.

Acknowledgments

We thank Dr. H. A. Fozzard for his advice and support and T. Kim and N. Adeeb for technical assistance.

References

1. Isom, L. L., K. S. De Jongh, and W. A. Catterall. Auxiliary subunits of voltage-gated ion channels. *Neuron* **12**:1183–1194 (1994).
2. Sutkowski, E. M., and W. A. Catterall. *Beta*-1 subunits of sodium channels: studies with subunit-specific antibodies. *J. Biol. Chem.* **265**:12393–12399 (1990).
3. Makita, N., P. B. Bennett, Jr., and A. L. George, Jr. Voltage-gated Na^+ channel *Beta*1 subunit mRNA expressed in adult human skeletal muscle, heart, and brain is encoded by a single gene. *J. Biol. Chem.* **269**:7571–7578 (1994).
4. Tong, J., J. F. Potts, J. M. Rochelle, M. F. Seldin, and W. S. Agnew. A single *beta*1 subunit mapped to mouse chromosome 7 may be a common component of Na channel isoforms from brain, skeletal muscle and heart. *Biochem. Biophys. Res. Commun.* **195**:679–685 (1993).
5. Isom, L. L., K. S. DeJongh, D. E. Patton, B. F. X. Reber, J. Offord, H. Charbonneau, K. Walsh, A. L. Goldin, and W. A. Catterall. Primary structure and functional expression of the $beta_1$ subunit of the rat brain sodium channel. *Science (Washington D. C.)* **256**:839–842 (1992).
6. Bennett, P. B., N. Makita, and A. L. J. George. A molecular basis for gating mode transitions in human skeletal muscle sodium channels. *FEBS Lett.* **326**:21–24 (1993).
7. Satin, J., J. W. Kyle, M. Chen, R. B. Rogart, and H. A. Fozzard. The cloned cardiac sodium channel α subunit expressed in *Xenopus* oocytes show gating and blocking properties of native channels. *J. Membr. Biol.* **130**: 11–22 (1992).
8. Nuss, H. B., N. Chiamvimonvat, M. T. Pérez-Garcia, G. F. Tomaselli, and E. Marban. Functional association of the β1 subunit with human cardiac and rat skeletal muscle (μ1) sodium channels expressed in *Xenopus* oocytes. *J. Gen. Physiol.*, in press (1995).
9. Gellens, M. E., A. L. George, Jr., L. Q. Chen, M. Chahine, R. Horn, R. L. Barchi, and R. G. Kallen. Primary structure and functional expression of the human cardiac tetrodotoxin-insensitive voltage-dependent sodium channel. *Proc. Natl. Acad. Sci. USA* **89**:554–558 (1992).
10. Hartmann, H. A., A. A. Tiedeman, S. F. Chen, A. M. Brown, and G. E. Kirsch. Effects of III-IV linker mutations on human heart Na^+ channel inactivation gating. *Circ. Res.* **75**:114–122 (1994).
11. Makielski, J. C., J. T. Limberis, S. Y. Chang, Z. Fan, and J. W. Kyle. Na channel β1 association with cardiac Na channel α subunits demonstrated by lidocaine block. *Biophys. J.* **68**:A157 (1995).
12. Wittenberg, B. A., and T. F. Robinson. Oxygen requirements, morphology, cell coat, and membrane permeability of calcium-tolerant myocytes from adult rat heart. *Cell. Tissue. Res.* **216**:231–251 (1981).
13. Chomczynski, P., and N. Sacchi. Single step method of RNA isolation by acid guanidinium thiocyanate-phenol-chloroform extraction. *Anal. Biochem.* **162**:156–159 (1987).
14. Bezanilla, F., and C. M. Armstrong. Inactivation of the sodium channel. I. Sodium current experiments. *J. Gen. Physiol.* **70**:549–566 (1977).
15. Hondeghem, L. M., and B. G. Katzung. Time- and voltage- dependent interaction of antiarrhythmic drugs with cardiac sodium channels. *Biochim. Biophys. Acta* **472**:373–398 (1977).
16. Hille, B. Local anesthetics: hydrophilic and hydrophobic pathways for the drug-receptor reaction. *J. Gen. Physiol.* **69**:497–515 (1977).
17. Bean, B. P., C. J. Cohen, and R. W. Tsien. Lidocaine block of cardiac sodium channels. *J. Gen. Physiol.* **81**:613–642 (1983).
18. Goldin, A. L. Accessory subunits and sodium channel inactivation. *Curr. Opin. Neurobiol.* **3**:272–277 (1993).
19. Starmer, C. F., V. V. Nesterenko, A. I. Undrovinas, A. O. Grant, and L. V. Rosenshtraukh. Lidocaine blockade of continuously and transiently accessible sites in cardiac sodium channels. *J. Mol. Cell. Cardiol.* **23**:73–83 (1991).
20. Chahine, M., L. Chen, R. Barchi, R. Kallen, and R. Horn. Lidocaine block of human heart sodium channels expressed in *Xenopus* oocytes. *J. Mol. Cell. Cardiol.* **24**:1231–1236 (1992).
21. Krafte, D. S., K. Davison, N. Dugrenier, K. Estep, K. Josef, R. L. Barchi, R. G. Kallen, P. J. Silver, and A. M. Ezrin. Pharmacological modulation of human cardiac Na^+ channels. *Eur. J. Pharmacol.* **266**:245–254 (1994).
22. Hille, B. *Ionic Channels of Excitable Membranes*, Ed. 2. Sinauer Associates, Sunderland, MA (1992).
23. Patlak, J. Sodium channel subconductance levels measured with a new variance-mean analysis. *J. Gen. Physiol.* **92**:413–430 (1988).
24. Provencher, S. W. A Fourier method for the analysis of exponential decay curves. *Biophys. J.* **16**:27–41 (1976).

Send reprint requests to: Dr. Jonathan C. Makielski, University of Wisconsin Hospitals and Clinics, Cardiology Section H6/349, 600 Highland Ave., Madison, WI 53792-3248.

MOL PHARM
MOLECULAR PHARMACOLOGY
aspet
Downloaded from molpharm.aspetjournals.org at Zhejiang University on December 1, 2012